ISSN 0023-1584, Kinetics and Catalysis, 2006, Vol. 47, No. 1, pp. 40–48. © MAIK "Nauka/Interperiodica" (Russia), 2006.
Original Russian Text N.S. Nesterenko, F. Thibault-Starzyk, V. Montouilliout, V.V. Yushchenko, C. Fernandez, J.-P. Gilson, F. Fajula, I.I. Ivanova, 2006, published in Kinetika i Kataliz, 2006, Vol. 47, No. 1, pp. 45–53.

HIGHLY ORGANIZED CATALYTIC SYSTEMS

The Use of the Consecutive Adsorption of Pyridine Bases and Carbon Monoxide in the IR Spectroscopic Study of the Accessibility of Acid Sites in Microporous/Mesoporous Materials

N. S. Nesterenko*, F. Thibault-Starzyk, V. Montouilliout**, V. V. Yushchenko*, C. Fernandez**, J.-P. Gilson**, F. Fajula***, and I. I. Ivanova***

** Moscow State University, Moscow, 119899 Russia*
*** LCS, UMR 6506 CNRS-ENSI, Caen, France*
**** LMCCCO, UMR 5618 CNRS-ENSCM, Montpellier, France*

Received October 12, 2004

Abstract—A new approach to the evaluation of the accessibility of acid sites in microporous/mesoporous materials is developed and tested using a series of dealuminated mordenites. This approach is based on an IR-spectroscopic study of the consecutive adsorption of substituted alkylpyridines (pyridine, 2,4,6-trimethylpyridine, and 2,4,6-triethylpyridine) and carbon monoxide. This method allowed us to determine the strength and number of acid sites with various degrees of accessibility. The adsorption of 2,4,6-triethylpyridine on various types of materials is studied. The extinction coefficients of alkylpyridines are determined using a McBain balance placed in a cell for IR-spectroscopic measurements.

DOI: 10.1134/S0023158406010071

Detailed information on the structure and character of active sites is required for designing efficient heterogeneous catalysts [1, 2]. Mass-transfer processes responsible for the transfer of reactant molecules to active sites have an enormous effect on the catalytic properties of porous systems [3]. The accessibility of acid sites has been studied insufficiently; for the most part, only the role of active sites localized on the outer surface of catalysts has been determined [4, 5]. This problem is of considerable interest in microporous/mesoporous materials, in particular, dealuminated mordenites.

Dealuminated mordenites are widely used as catalysts for the isomerization of alkanes [6, 7], the synthesis of cumene [8], the alkylation of condensed aromatic hydrocarbons [9], and the transalkylation [10] and disproportionation [11] of alkylaromatic hydrocarbons. At the same time, commercially synthesized mordenites as catalytic materials exhibit a very important disadvantage: the quasi-one-dimensional system of channels hinders the diffusion of reactants to active sites, which are arranged in extended narrow channels, and reaction products from these sites. Therefore, the development of effective methods for studying the accessibility of acid sites in these catalysts is a key problem in the structural design of catalytic systems based on these zeolites. This problem is of particular importance for catalytic reactions with the participation of bi- and polynuclear aromatic compounds, whose molecular size and shape are crucial factors in the rates and directions of their chemical reactions in microporous zeolites.

The aim of this work was to develop a new approach to the evaluation of the accessibility of acid sites in microporous/mesoporous materials based on an IR-spectroscopic study of the consecutive adsorption of substituted alkylpyridines and carbon monoxide, which also provides an opportunity to determine the strength and amount of acid sites with various degrees of accessibility.

EXPERIMENTAL

Catalyst Preparation

CBV10 wide-pore mordenite (MOR) in the sodium form with the atomic ratio Si/Al = 7.6 (from Zeolyst) was used as the starting mordenite sample for catalyst preparation by dealumination. Before dealumination, the Na/MOR sample was converted into the ammonium form by triple ion exchange with a 0.1 M NH_4NO_3 solution at 70–80°C (20 ml of the solution per gram of zeolite (MOR)). Next, the zeolite was dried (80°C; 24 h) and calcined at 450°C (heating rate of 1 K/min) in flowing air for 8 h to prepare the H-form. The H-form (MOR) was dealuminated by acid treatment with 6 M methanesulfonic acid at 110°C (MOR-M) or by a combination of precalcination at 750°C followed by acid treatment with 2 M methanesulfonic acid at 110°C

Table 1. Characteristics of catalysts

Sample	Treatment procedure	Si/Al	Porosity		
			V_{micro}	V_{total}	S_{meso}
			cm^3/g		m^2/g
MOR	–	7.6	0.19	0.23	22
MOR-M	CH_3SO_2OH	49	0.20	0.26	44
MOR-750M	750°C + CH_3SO_2OH	79	0.23	0.30	53

(MOR-750M). Table 1 summarizes the properties of the resulting samples.

The sample of γ-Al_2O_3 was obtained by the calcination of boehmite at 550°C (S_{sp}^{BET} = 180 m^2/g), and the mesoporous material of the AlMCM-41 type (Si/Al = 39; S_{sp}^{BET} = 514 m^2/g) was synthesized in accordance with a procedure described elsewhere [12].

Characterization

The elemental analysis of the resulting samples (Al, Si) was performed by atomic absorption spectrometry at Service Central d'Analyses du CNRS (Vernaison, France).

The pore structure of the samples was studied by the low-temperature adsorption of nitrogen on ASAP-2000 (Micromeritics). The total adsorption pore volume (V_{total}) was calculated from the amount of nitrogen adsorbed at the relative pressure p/p_0 = 0.945 in the adsorption branch of the isotherm, and it corresponded to the volume of sample pores with a diameter smaller than 300 Å [13]. The *t*-plot method of De Boer and Lippens [14, 15] was used for determining the micropore volume (V_{micro}) and mesopore surface area (S_{meso}).

NMR spectra were measured on a Bruker Avance 400 spectrometer with a magnetic field of 9.4 T, which corresponds to the working frequencies $\nu(^1H)$ = 400.33 and $\nu(^{27}Al)$ = 104.23 MHz. The DM2003 program was used in the processing of spectra.

The ^{27}Al NMR spectra were recorded for air-dry samples using magic angle spinning (54.7°) at a frequency of 14 kHz with a 4-mm ZrO_2 rotor. A 1 M $Al(NO_3)_3$ solution was used as the reference for determining chemical shifts (δ). The recycle delay in a pulse sequence was 0.5 s.

To measure the NH_3 TPD spectra, the test sample ~0.1 g in weight with a particle size of 0.5–0.25 mm was placed in a quartz reactor between the beds of quartz with a particle size of 1–0.5 mm. The sample was treated with flowing dry air at 550°C for 1 h followed by blowing with nitrogen. Saturation was performed in a flow of dried ammonia diluted with nitrogen (1 : 20) at room temperature for 30 min. Physically adsorbed ammonia was removed in a flow of dry helium at 100°C for 1 h. To obtain a TPD curve, the temperature was increased to 700°C at a rate of 8 K/min. The signals from the katharometer and the temperature sensor were measured simultaneously through a multichannel analog-to-digital converter using the Ecochrom program. The TPD spectra of NH_3 were calculated in accordance with a procedure described elsewhere [16].

IR spectra were measured on a Protege 460 Fourier transform spectrometer (Nicolet) with an MCT detector. The OMNIC ESP version 6.0 program was used in data processing. The spectra were recorded with a resolution of 4 cm^{-1} over the range 4000–400 cm^{-1}.

The combined adsorption of CO and a pyridine base was performed in the same pellet in a cell for low-temperature measurements [17, 18]. After a standard sample pretreatment, the adsorption of CO at –196°C was performed in accordance with a published procedure [19]. Next, the sample was heated to room temperature for CO desorption; thereafter, an alkylpyridine was adsorbed at 180°C. After the saturation of the surface with the alkylpyridine, the sample was cooled to –196°C once again and the adsorption of CO was repeated.

A system described in [20] was used in measuring the extinction coefficients of pyridine (Py), 2,4,6-trimethylpyridine (Me_3Py), and 2,4,6-triethylpyridine (Et_3Py) probe molecules. In this system, the IR cell was equipped with the McBain balance, a temperature controller, and a pressure gage. This allowed us to perform the simultaneous control of weight, temperature, and pressure and to measure IR spectra. The sample weight was measured on a McBain balance with an accuracy of 10^{-2} mg. Before experiments, the samples were activated at 450°C for 10 h. The amount of probe molecules adsorbed on the sample was varied by stepwise desorption over the temperature range 150–350°C. The standard procedure consisted in raising the temperature to a specified value, heating the sample at this temperature for 5 min, and measuring the IR spectra after cooling the sample to 150°C. The temperature was increased in steps of 25°C. As a result, the dependence of band intensity on adsorbate amount was obtained,

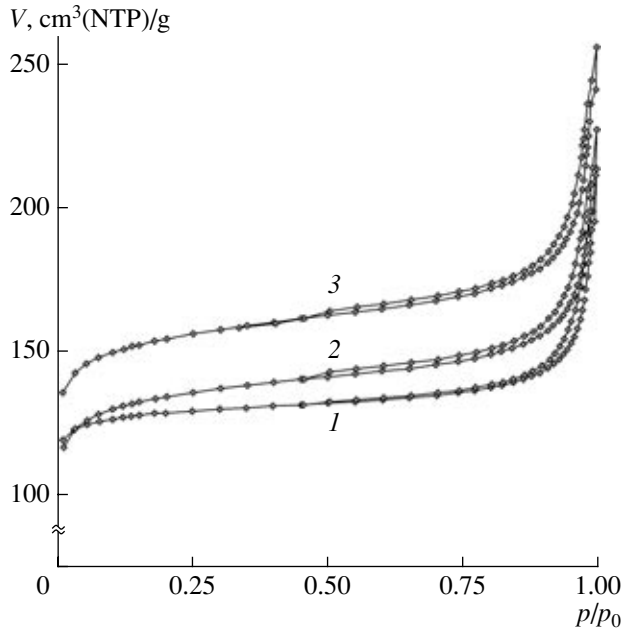

Fig. 1. Isotherms of the low-temperature adsorption–desorption of nitrogen on (*1*) MOR, (*2*) MOR-M, and (*3*) MOR-750M.

from which the extinction coefficient (ε) was calculated by the equation

$$\varepsilon = AS/n, \quad (1)$$

where A (cm^{-1}) is the corresponding absorption band intensity, S (cm^2) is the surface area of a pellet, and n (μmol) is the amount of the adsorbate substance.

The extinction coefficients for dealuminated mordenites were the following: $\varepsilon(B)_{1545}$ = 1.02 and $\varepsilon(L)_{1454}$ = 0.89 cm/μmol for Py; $\varepsilon(Me_3Py)_{1632–1648}$ = 10.1 cm/μmol; and $\varepsilon(Et_3Py)_{1632–1648}$ = 10.5 cm/μmol.

RESULTS AND DISCUSSION

It is well known that the micropore system of mordenite includes main channels and side pockets. The main channels are formed by 12-membered quasi-elliptical rings (6.5 × 7.0 Å), and they account for 57% of the total micropore volume [21, 22]. Lateral or side pockets are arranged perpendicularly in the walls of main channels. Each side pocket is joined to the main channel and two side pockets in the walls of a neighboring main channel through eight-membered rings. The side pockets have the shape of a prism, and they are formed by two eight-membered rings of sizes 3.7 × 4.8 Å at the main channel entrance and 5.7 × 2.6 Å at the boundary between each other. Because of these limitations, it is practically impossible for the majority of molecules to pass from one main channel to another. For this reason, mordenite can be considered as a one-dimensional system of main channels without taking into account side pockets.

Structural studies demonstrated that the parent mordenite had three localization places of acid sites, which are formed by bridging OH groups. Of the ten crystallographic positions of oxygen in the mordenite structure, only three positions participate in the formation of acidic OH groups with equal occupancies: O7 in main channels, O2 at the boundary between main channels and side pockets, and O9 in side pockets [23, 24]. Thus, in the ideal mordenite structure, 2/3 of acid sites occur in main channels and 1/3, in side pockets. Previously [22, 25, 26], it was found that the sites in side pockets are inaccessible to pyridine, benzene, or cyclohexane. Bulkier molecules, such as trimethylbenzene, practically do not penetrate into the system of main channels in mordenite [24].

Dealumination significantly changed the pore structure of the parent mordenite. Figure 1 shows the nitrogen adsorption isotherms for MOR, MOR-M, and MOR-750M. The isotherms observed in dealuminated mordenites are much different from those for the parent sample. According to the IUPAC classification, they can be assigned to the mixed type I + IV, which suggests the simultaneous presence of micropores and mesopores in the sample [27]. Quantitative data on calculated isotherms, which are given in Table 1, indicate that dealumination by acid treatment resulted in the appearance of mesopores and in an increase in the outer surface area. The micropore volume remained practically unchanged after this treatment. In contrast, calcination combined with the subsequent acid treatment resulted in an increase in both the micropore volume and the outer surface area of the samples.

The ^{27}Al NMR spectra of the dealuminated samples show a single signal at δ = 55 ppm, which corresponds to tetrahedrally coordinated aluminum atoms (Fig. 2). Thus, all of the aluminum atoms occurred in the zeolite framework.

According to chemical analysis data, the aluminum content of the samples strongly decreased as a result of dealumination (Tables 1, 2). This is also evidenced by a decrease in the amount of desorbed ammonia in NH_3 TPD experiments (Table 2, Fig. 3). In addition to information on the total amount of acid sites, the NH_3 TPD method allowed us to determine the strength distribution of acid sites [16]. Figure 3 shows the NH_3 TPD curves for parent and dealuminated samples. An analysis of these curves demonstrated that the dealumination of mordenites did not result in a considerable change in the strength distribution of acid sites. In all cases, two desorption peaks were observed, and the positions of peak maximums remained practically unaffected. However, the removal of aluminum from the mordenite structure changed the distribution density and accessibility of acid sites [10, 19, 28].

A new approach [19] based on the consecutive adsorption of pyridine bases and carbon monoxide was developed for studying the accessibility of Brønsted acid sites in narrow-pore mordenites. However, for

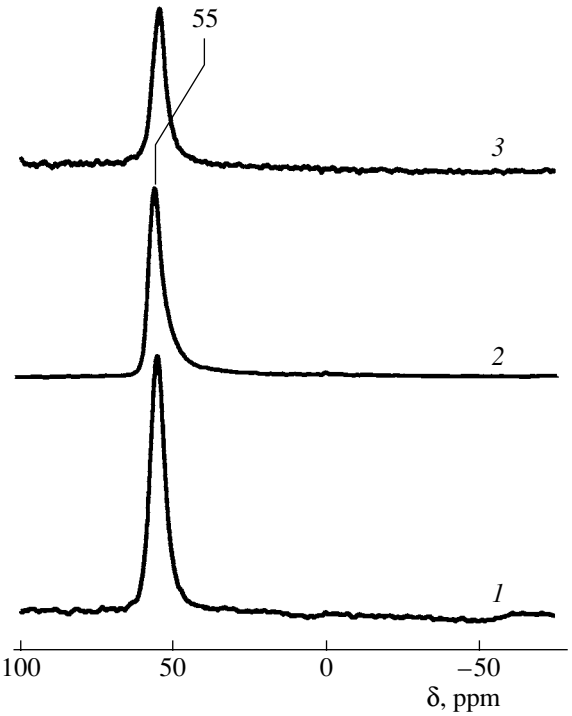

Fig. 2. ^{27}Al NMR spectra of (*1*) MOR, (*2*) MOR-M, and (*3*) MOR-750M.

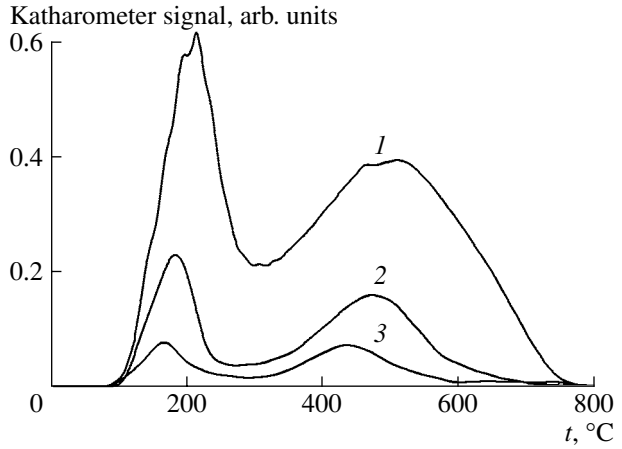

Fig. 3. NH_3 TPD spectra of the samples (*1*) MOR, (*2*) MOR-M, and (*3*) MOR-750M.

studying microporous/mesoporous materials based on zeolites, it was necessary to use a wider range of alkylpyridine bases (Py, Me_3Py, and Et_3Py). These probe molecules were chosen because of the structure peculiarities of zeolites and microporous/mesoporous materials. In the majority of zeolite materials, micropore entrances are 8-, 10-, or 12-membered rings. The molecular size of pyridine is such that the molecule cannot penetrate through eight-membered rings but penetrates through ten-membered rings. In turn, Me_3Py and Et_3Py molecules cannot penetrate through 10- and 12-membered rings, respectively, and cannot interact with oxygen sites localized in these types of channels within the zeolite structure. Therefore, Me_3Py can be used for a selective study of acid sites in zeolite channels with windows containing 12-membered rings, whereas Et_3Py can be used for acid sites in micropore mouths and mesopores. Note that, in this work, we used Et_3Py as a probe molecule in IR spectroscopy for the first time.

The proposed approach includes the following three stages:

(1) the adsorption and desorption of carbon monoxide and recording the spectrum of adsorbed CO on a freshly activated sample;

(2) the adsorption of a pyridine base;

(3) the adsorption of CO on the sample with the preadsorbed pyridine base and recording the spectrum of adsorbed CO.

The adsorption and desorption of carbon monoxide was performed in order to study the nature and strength of all acid sites in the sample. At the second stage, the fraction of OH groups and the total amount of acid sites that interact with the pyridine base and, consequently,

Table 2. Amount of acid sites on dealuminated mordenites

Sample	Si/Al	N_{Al}	N_{NH_3}	N_{Py}	B/L	N_{Me_3Py}	N_{Et_3Py}
		μmol/g	μmol/g	μmol/g		μmol/g	μmol/g
MOR	7.6	1970	1380	1100	2.7	203	113
MOR-M	49	330	370	300	5.6	125	25
MOR-750M	79	210	160	210	2.7	161	147

Note: N_{Al} is the amount of aluminum atoms on the catalyst determined from chemical analysis data; N_{NH_3} is the amount of acid sites measured by the NH_3 TPD method; N_{Py} is the amount of acid sites measured by the IR spectroscopy of adsorbed probe molecules; B/L is the ratio between the numbers of Brønsted and Lewis sites.

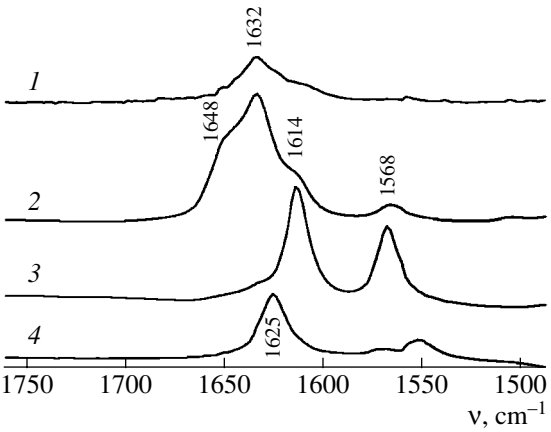

Fig. 4. IR spectra of Et_3Py on the following samples: (*1*) AlMCM-41 at 180°C, (*2*) MOR-750M at 180°C, (*3*) MOR-750M at room temperature, and (*4*) Al_2O_3 at 180°C.

the accessibility of sample sites to this base were determined. The additional adsorption of CO gave information on the nature and strength of acid sites that are inaccessible to the chosen pyridine base. A sequential increase in the size of probe molecules in a series of experiments resulted in the gradual liberation of a portion of sites for interaction with CO; this allowed us to obtain information on the nature and strength of sites with different accessibilities.

The IR spectra of alkylpyridine bases adsorbed at acid sites of various types differed in the positions of absorption bands in the region of aromatic ring vibrations. For the assignment of absorption bands, we performed the adsorption of Et_3Py on materials with sites of various natures:

(1) Al-MCM-41, a mesoporous aluminosilicate material, which primarily possesses Lewis acid sites;

(2) γ-Al_2O_3, a mesoporous/macroporous material, which primarily possesses Lewis acid sites but does not contain silicon;

(3) MOR-750M, a microporous/mesoporous material, which contains both Lewis and Brønsted acid sites and a large amount of silanol groups.

The adsorption of Et_3Py on activated Al-MCM-41 at 180°C resulted in the appearance of an absorption band at 1632 cm^{-1}, which corresponds to the interaction of the probe molecule with Lewis acid sites on the mesoporous aluminosilicate material (Fig. 4). Note that the position of the absorption band of Et_3Py adsorbed at the Lewis acid sites of γ-Al_2O_3 was different. The band at 1625 cm^{-1} in the spectrum of adsorbed Et_3Py corresponds to its interaction with Lewis acid sites in aluminum oxide, whereas the band at 1632 cm^{-1} corresponds to the interaction with coordinatively unsaturated aluminum atoms in the aluminosilicate structure, which are formed as a result of dehydroxylation in the course of sample activation. The molecular size of Et_3Py is such that this compound practically did not penetrate into the pore system of mordenite at room temperature. Thus, it is likely that its adsorption on the sample MOR-750M at room temperature, which gave rise to a band at 1614 cm^{-1}, was due to the interaction of this probe molecule with silanol groups or physically adsorbed Et_3Py (Fig. 4). After heating to 180°C, the shape of the spectrum of Et_3Py adsorbed on MOR-750M changed dramatically; the absorption bands due to physisorbed Et_3Py disappeared and two bands appeared at 1648 and 1632 cm^{-1}. As demonstrated above, the band at 1632 cm^{-1} corresponds to adsorption at Lewis acid sites. The appearance of absorption bands at 1648 cm^{-1} and the simultaneous disappearance of the absorption band due to bridging OH groups allowed us to attribute this band to Et_3Py adsorbed at Brønsted acid sites (Fig. 4). The interpretation of the bands in the IR spectra of Me_3Py was analogous. The absorption bands at 1632 and 1648 cm^{-1} were subsequently used for the quantitative evaluation of the accessibility of acid sites with consideration for the found extinction coefficients.

Figure 5 shows the IR spectra of the OH groups of mordenites from the MOR series before and after adsorption of pyridine bases (Py, Me_3Py, and Et_3Py) and the IR spectra obtained after the subsequent adsorption of CO on the surface of MOR before and after its interaction with bulky probe molecules. The bands at 2138 and 2157 cm^{-1} and in the region 2170–2180 cm^{-1} correspond to unbound CO and CO molecules adsorbed at silanol groups and Brønsted acid sites, respectively; the bands at 2210 and 2226 cm^{-1} correspond to CO molecules coordinatively bound to strong and weak Lewis sites, respectively [19]. It can be seen in Fig. 5a that the OH groups of the parent mordenite MOR remained practically intact after the adsorption of Et_3Py and Me_3Py and the intensity of adsorption bands in the IR spectra decreased only slightly. Note that the absorption frequency characteristic of the poisoning of all of the OH groups in the main channels of mordenite [19, 22] was not shifted. This suggests that the bulky probe molecules interact only with acidic OH groups on the outer surface or at pore mouths rather than penetrate into the pores of mordenite. Noticeable changes in the spectrum of OH groups and a shift of their absorption bands to the region of smaller wave numbers appeared only after the adsorption of pyridine. This is indicative of the interaction of pyridine with OH groups that are localized only in the main channels. Analogously, Fig. 5b exhibits only an insignificant decrease in the absorption band of CO (2175 cm^{-1}) bound to Brønsted acid sites after poisoning with Me_3Py and Et_3Py. At the same time, the interaction with pyridine resulted in considerable changes and a shift of this band from 2175 to 2170 cm^{-1}, which corresponds to the interaction of CO with hydroxyl groups localized in side pockets (Fig. 5b). Thus, the fraction of Brønsted sites localized in side pockets can be determined from the IR spectra of OH groups after pyridine adsorption. The total amount of acid sites in

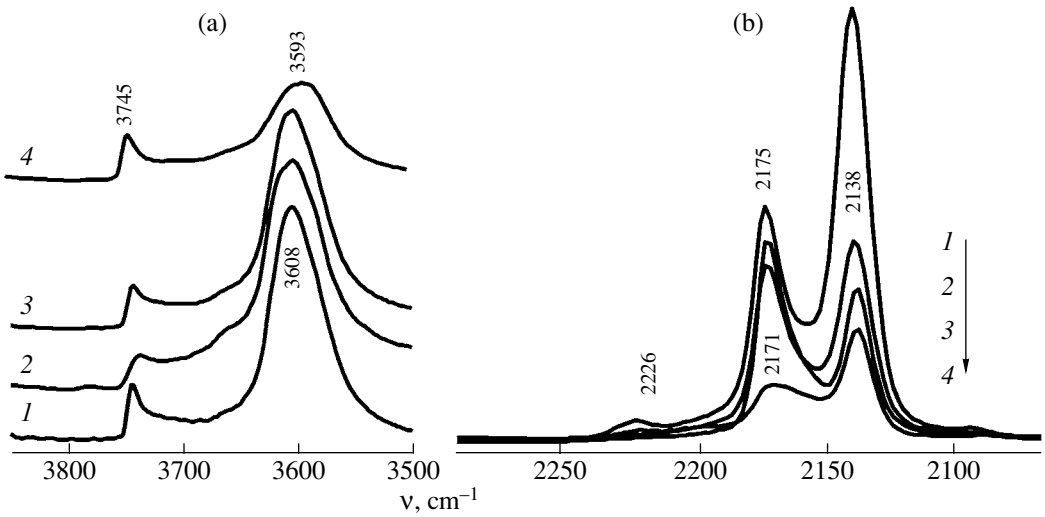

Fig. 5. IR spectra of the sample MOR in the region of absorption due to OH groups: (a) (*1*) activated sample, after the adsorption of (*2*) Et_3Py, (*3*) Me_3Py, and (*4*) Py; (b) after the subsequent adsorption of CO on (*1*) the initial sample (+CO), (*2*) after Et_3Py (+Et_3Py + CO), (*3*) after Me_3Py (+Me_3Py + CO), and (*4*) after Py (+ Py + CO).

the main and side pockets of mordenite can be determined using the extinction coefficients of pyridine measured with the use of a McBain balance (Tables 2, 3). With consideration for the difference between the extinction coefficients for the absorption bands of OH groups in main (ε_{mp}) and side pockets (ε_{lp}) ($\varepsilon_{mp}/\varepsilon_{lp} \sim 1.5$), which was found by Makarova *et al.* [25], the amount of accessible sites measured using pyridine adsorption is in good agreement with that obtained from the IR spectrum of OH groups before and after pyridine adsorption.

Information on the nature and strength of acid sites inaccessible to various probe molecules can be obtained from the IR spectra of adsorbed CO (Table 4). It can be seen in Table 4 that the Brønsted OH groups inaccessible to pyridine and localized in the side pockets exhibit weaker acid properties than the sites in main channels. Aluminum that generated the strongest acid sites was extracted last in the course of dealumination. Therefore, as the accessibility of the centers increased, the average strength of the centers increased, as measured using CO adsorption (Table 4). These results are consistent with published data [3, 22, 29], and they suggest that the most accessible OH groups in mordenite-type zeolites are the strongest acid sites. Note that the band at 2226 cm^{-1}, which corresponds to adsorption at strong Lewis acid sites, disappeared after the adsorption of any one of the probe molecules. This provides additional support to the hypothesis that this type of Lewis sites results from the dehydroxylation of Brønsted acid sites. It is quite reasonable that the sites on the outer surface and the most accessible sites are primarily prone to dehydroxylation. It is of interest that the acid properties of silanol groups before and after surface poisoning with probe molecules remained unchanged in the parent mordenite; this suggests that they are uniform.

According to the data obtained by the low-temperature adsorption of nitrogen, the treatment of MOR with methanesulfonic acid resulted in the appearance of mesopores in the sample. In this case, all of the acid sites became accessible to pyridine (Fig. 6; Tables 2, 3). However, as a result of this treatment, only about a half of the sites became accessible to Me_3Py, whereas the acid sites were practically inaccessible to Et_3Py (Fig. 6; Tables 2, 3). Interestingly, the strengths of accessible and inaccessible Brønsted acid sites were practically equal in this sample (Table 4).

The dealumination of MOR by calcination followed by treatment with methanesulfonic acid resulted in the full accessibility of all of the sites regardless of probe molecules (Fig. 7; Tables 2, 3). No acid sites capable of interacting with CO remained after the adsorption of pyridine bases. The amount of acid sites determined with the use of extinction coefficients for alkylpyridines was equal to the number of sites obtained from NH_3 TPD data.

Table 3. Amount of accessible OH groups (%) on dealuminated mordenites

Sample	+Py	+Me_3Py	+Et_3Py
MOR	55	10	5
MOR-M	100	80	30
MOR-750M	100	100	100

Table 4. Strength of acid sites in dealuminated mordenites

Sample	$\langle E \rangle^*_{NH_3}$, kJ/mol	CO	+Py + CO	+Me_3Py + CO	+Et_3Py + CO
		Δν(CO–HO), cm^{-1}			
		SiO(H)Al	SiO(H)Al	SiO(H)Al	SiO(H)Al
MOR	182	335	300	323	333
MOR-M	172	319	–	320	320
MOR-750M	175	330	–	–	–

* Average activation energy of ammonia desorption above 250°C.

Thus, the treatment of original mordenite with methanesulfonic acid decreased the average strength of acid sites, whereas calcination followed by acid treatment only slightly affected the strength of acid sites (Table 4). This was likely due to the nonuniform extraction of aluminum from the samples. It is likely that the treatment with methanesulfonic acid resulted in the predominant extraction of aluminum from the outer surface and main channels of mordenite. This is explained by the fact that this acid forms bulky compounds with aluminum. Thus, the treatment with methanesulfonic acid can result in a nonuniform distribution of aluminum, and it does not ensure the removal of aluminum from side pockets. In contrast, thermal pretreatment caused the rupture of Si–O–Al bonds, and the removal of aluminum occurred more uniformly in this case.

Table 3 summarizes quantitative data on the accessibility of Brønsted acid sites to alkylpyridines. The fractions of sites accessible to various alkylpyridines were calculated as the ratio of the change in the OH band intensity upon the adsorption of a base to the change in the OH band intensity upon CO adsorption. In original MOR, about 55% of sites were accessible to pyridine molecules; this corresponds to sites localized in main channels. Only about 10% of sites, which were likely arranged on the outer surface and in zeolite pore mouths, were accessible to bulkier probe molecules (Me_3Py and Et_3Py). The acid treatment of MOR made all of the acid sites accessible to pyridine and signifi-

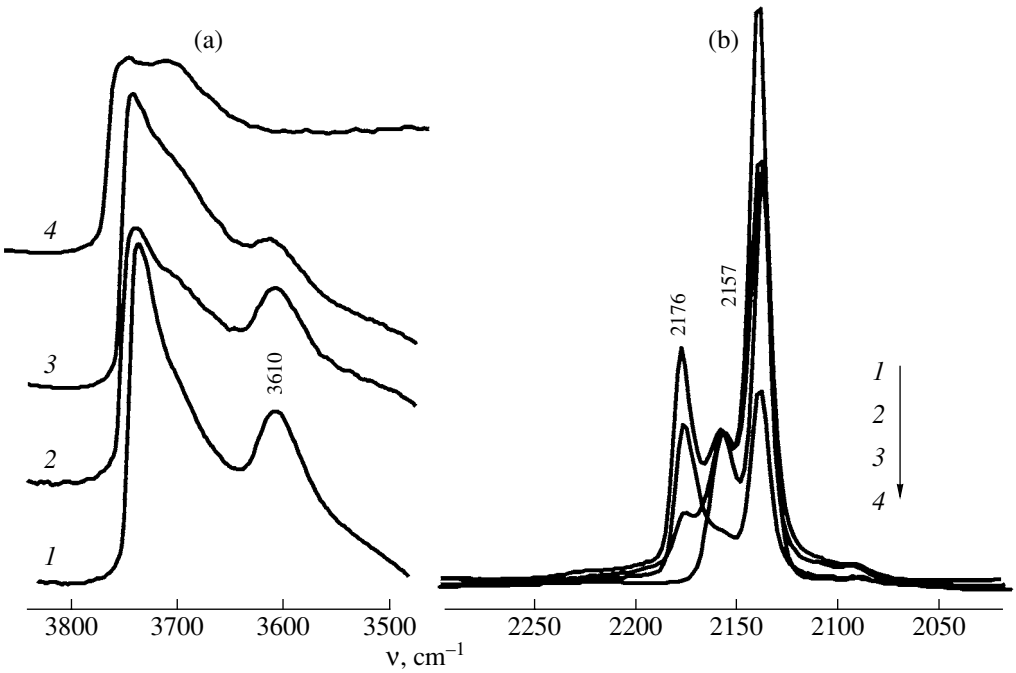

Fig. 6. IR spectra of MOR-M in the region of absorption due to OH groups: (a) (*1*) activated sample, after the adsorption of (*2*) Et_3Py, (*3*) Me_3Py, and (*4*) Py; (b) after the subsequent adsorption of CO on (*1*) the initial sample (+CO), (*2*) after Et_3Py (+Et_3Py + CO), (*3*) after Me_3Py (+Me_3Py + CO), and (*4*) after Py (+Py + CO).

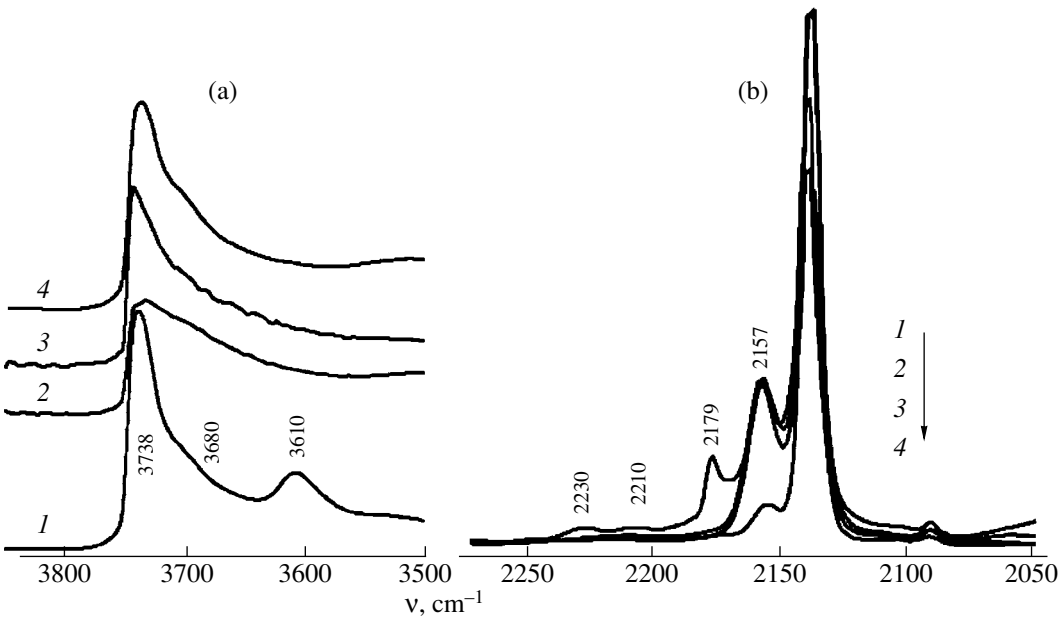

Fig. 7. IR spectra of the sample MOR-750M in the region of absorption due to OH groups: (a) (*1*) activated sample, after the adsorption of (*2*) Et_3Py, (*3*) Me_3Py, and (*4*) Py; (b) after the subsequent adsorption of CO on (*1*) the initial sample (+CO), (*2*) after Et_3Py (+Et_3Py + CO), (*3*) after Me_3Py (+Me_3Py + CO), and (*4*) after Py (+Py + CO).

cantly increased the accessibility of sites to Me_3Py and Et_3Py. Calcination combined with acid treatment resulted in that all of the acid sites became fully accessible to all of the three molecules. This conclusion is consistent with the appearance of a secondary pore system, which is responsible for the free transport of bulky molecules.

Thus, in this work, we developed a new approach to studies of acid sites with various degrees of accessibility in microporous/mesoporous materials prepared based on dealuminated mordenites. The procedure is based on an IR spectroscopic study of the consecutive adsorption of pyridine bases and carbon monoxide. We found that Et_3Py can be used as a probe molecule for the IR-spectroscopic study of the accessibility of acid sites in microporous/mesoporous materials. The extinction coefficients of Py, Me_3Py, and Et_3Py were measured with a McBain balance coupled with an IR-spectroscopic cell. This method allowed us to obtain information on the amount and strength of acid sites with different accessibilities.

ACKNOWLEDGMENTS

N.S. Nesterenko acknowledges the support of a NATO Reintegration Grant and the Foundation for Support of Domestic Science.

REFERENCES

1. Soler-Illia, G.J., Sanchez, C., Lebeau, B., and Patarin, J., *Chem. Rev.*, 2002, vol. 102, p. 4093.
2. Brunel, D., Blanc, A., Galarneau, A., and Francois, F., *Catal. Today*, 2002, vol. 73, nos. 1–2, p. 139.
3. McQueen, D., Chiche, B., Fajula, F., *et al.*, *J. Catal.*, 1996, vol. 161, no. 2, p. 587.
4. Corma, A., Fornes, V., Forni, L., *et al.*, *J. Catal.*, 1998, vol. 179, no. 2, p. 451.
5. Creyghton, E.J., Elings, J.A., Downing, R.S., *et al.*, *Microporous Mater.*, 1996, vol. 5, no. 5, p. 299.
6. Li, C.L., Novaro, O., Munoz, E., *et al.*, *Appl. Catal., A*, 2000, vol. 199, no. 2, p. 211.
7. Liu, H., Lei, G.D., and Sachtler, W.M.H., *Appl. Catal., A*, 1996, vol. 137, no. 1, p. 167.
8. Perego, C., Amarilli, S., Bellussi, G., *et al.*, *Microporous Mater.*, 1996, vol. 6, nos. 5–6, p. 395.
9. Song, C., *C. R. Acad. Sci., Ser. 2c*, 2000, vol. 3, p. 477.
10. Nesterenko, N.S., Timoshin, S.E., Kuznetsov, A.S., *et al.*, *Stud. Surf. Sci. Catal.*, 2004, vol. 154, p. 2163.
11. Mishin, I.V., Beyer, H.K., and Karge, H.G., *Appl. Catal., A*, 1999, vol. 180, nos. 1–2, p. 207.
12. Nesterenko, N.S., Ponomoreva, O.A., and Yuschenko, V.V., *Appl. Catal., A*, 2003, vol. 254, no. 2, p. 261.
13. Broekhoff, J. and de Boer, J., *J. Catal.*, 1967, vol. 9, p. 15.
14. Lippens, B.C. and De Boer, J.H., *J. Catal.*, 1965, vol. 4, p. 319.
15. Gregg, S.J. and Sing, K.S.W., *Adsorption, Surface Area, and Porosity*, London: Academic, 1967.

16. Yushchenko, V.V., *Zh. Fiz. Khim.*, 1997, vol. 71, no. 4, p. 628.
17. Tsyganenko, A.A., *Prib. Tekh. Eksp.*, 1980, vol. 1, p. 255.
18. Mauge, F., Lamotte, J., Nesterenko, N.S., *et al.*, *Catal. Today*, 2001, vol. 70, nos. 1–3, p. 271.
19. Nesterenko, N.S., Thibault-Starzyk, F., Montouilliout, V., *et al.*, *Microporous Mesoporous Mater.*, 2004, vol. 71, nos. 1–3, p. 157.
20. Thibault-Starzyk, F., Gil, B., Aiello, S., *et al.*, *Microporous Mesoporous Mater.*, 2004, vol. 67, p. 107.
21. Meier, W.M., *Z. Kristallogr.*, 1961, vol. 115, p. 439.
22. Maache, M., Janin, A., Lavalley, J.C., and Benazzi, E., *Appl. Spectrosc.*, 1995, vol. 15, no. 6, p. 507.
23. Alberti, A., *Appl. Spectrosc.*, 1997, vol. 19, nos. 5–6, p. 411.
24. Nesterenko, N.S., *Cand. Sci. (Chem.) Dissertation*, Moscow: Moscow State Univ., 2003.
25. Makarova, M.A., Wilson, A.E., van Liemt, B.J., *et al.*, *J. Catal.*, 1997, vol. 172, no. 1, p. 170.
26. Zholobenko, V.L., Makarova, M.A., and Dwyer, J., *J. Phys. Chem.*, 1993, vol. 97, no. 22, p. 5962.
27. IUPAC, *Pure Appl. Chem.*, 1994, vol. 66, no. 8, p. 1739.
28. Zholobenko, V.L. and Mitchell, G.P., *Stud. Surf. Sci. Catal.*, 2001, vol. 135, p. 220.
29. Farcasiu, D., Leu, R., and Corma, A., *J. Phys. Chem. B*, 2002, vol. 106, no. 5, p. 928.